PRODUCTION TEST OF ENERGY DOUBLER MAGNETS

R. Yamada, M. E. Price, and D. A. Gross

Fermi National Accelerator Laboratory
Batavia, Illinois

SUMMARY

The test results of Energy Doubler/Saver bending magnets, especially three of the E22-14 series, are presented. Each is tested with forced flow liquid helium in its own cryostat with warm iron laminations, using a prototype satellite refrigerator. The following characteristics were measured for each magnet: training behavior, ac loss, field quality using harmonic analysis, and absolute field value using an NMR. A stretched wire loop was used to measure the vertical plane and integrated field value. The end field values are also measured using harmonic analysis and a Hall probe. The production test facility under construction will also be reported. The major components are a CTI 1500 refrigerator, a helium distribution box, six magnet test stands and the overall control unit, and a data acquisition system for magnet test. Their characteristics are described. This will allow production testing of Energy Doubler/Saver magnets at the rate of three a day.

INTRODUCTION

In the past several years, development on the Energy Doubler/ Saver magnets has continued[1]. Up to now several different types of prototype bending magnets were developed (B-, C-, D-, and E-series) in one, five, and ten-foot models. In the past year production of twenty-two foot bending magnets was started. The final

type of coils for bending magnets is now E-series, and up to now two types of cryostats have been developed: E22-1 and E22-14 series. Ten E22-1 series magnets have been made, and two have been measured for their magnetic field characteristics and reported[2-3].

While eleven E22-14 series magnets have been produced, three have been measured: E22-15, -19, and -33. In the first part of this paper their magnetic characteristics will be reported. Before the assembly of coils into the cryostat, the Energy Doubler/Saver Group tested each coil in a slanted dewar using pool boiling liquid helium. They also tested a string of assembled magnets for operational characteristics[4].

In the second part of this paper, the production test facility for testing all of the Energy Doubler/Saver production bending and quadrupole magnets will be described. The facility is now under construction and it will be operational this fall. The total number of magnets needed and to be tested for the Energy Doubler/Saver is 774 twenty-two foot bending magnets and 180 five-foot quadrupole magnets. To test all these magnets in a reasonable time and with a minimum of personnel, a very efficient testing facility with a fully automated system is required. The basic characteristics of the components and their functions are presented.

E22-14 SERIES MAGNETS

The cross section of the E22-14 series bending magnets is shown in Fig. 1. The outside dimensions of the magnets are 10 inches by 15 inches. The coils of the E22-1 and the E22-14 series magnets are basically the same, but there are several

changes in their cryostats. The collars which hold the coils in place against the magnetic force have been changed from type 1 to type 4, allowing improved Helium cooling efficiency. A nitrogen shield was incorporated into the cryostat instead of the 20°K He gas line. The two-phase Helium passage was moved outside the coil structure to intercept incoming heat. Accordingly, the size of beam bore tube was increased to a width of 2.810 inches, and the shape is now a square which has been positioned to give the maximum horizontal and vertical aperture. The size of the roller suspension was reduced. The connecting parts at the end of the magnet were rearranged as shown in Fig. 2.

MAGNET MEASUREMENTS

The magnets to be reported here are E22-15, -19, and -33, which are E22-14 series magnets. They were measured using the same prototype satellite refrigerator and the same data acquisition system, based on a PDP-11/10 and CAMAC system, as was used for E22-13[3].

Quench

A typical load line is shown in Fig. 3. The maximum field values obtained with and without iron are 43.1 and 41.9 kG. All three magnets exceeded 40 kG at center. Design field is 42.3 kG at 4.6°K at the center of the magnet. Due to refrigeration problems the single phase Helium temperature varied from .2 to .4°K above the design value. This lowered the maximum attainable field by 4 to 8%.

During a quench the pressure in the single phase Helium, the current, and the voltage across the magnet are monitored. The magnet resistance, energy loss in the magnet and upper limit of the coil temperature are calculated.

AC Loss

The ac loss of the magnets was measured as a function of maximum field and also as a function of ramp rate. Typical curves for ac loss versus current starting at zero field and at 9 kG are shown in Fig. 4. Once above the flux penetration field (~1 kG), the losses should be roughly linear with increasing field. This is very close to the case up to about 25 kG, where the losses start increasing more rapidly. The increase in energy loss above 25 kG indicates an inelastic mechanical movement within the coil. If this increase did not occur, then the loss at 42.3 kG (1000 GeV) would be about 600 Joules (or about 10 watts/magnet) for a one-minute cycle. For a cycle between 4.2 kG (100 GeV) and 42.3 kG (1000 GeV), the energy loss (i.e. heat dissipated in the Helium) is about 50 Joules less than the loss for a cycle starting at 0 kG. Magnetization curves were also plotted and these showed a pronounced downward droop at high field. This implies a coil deformation agreeing with the loss data. In addition, the curve starts turning upward above 40 kG, indicating some saturation in the iron laminations.

Field Homogeneity Measurement with NMR

The central field of each magnet was measured using an NMR circuit and a signal averager[5]. At fields below 20 kG and using a proton sample it was possible to obtain a clean signal. However, at higher fields where a lithium sample is necessary the S/N ratio was low.

One magnet was measured at a current of 2000 A at 6" intervals along its entire length. The field fluctuated by 0.15% along

the magnet axis. The data is shown in Fig. 5. Additional measure-
ments showed these fluctuations to be reproducible. These are
probably caused by small irregularities in the production accuracy
of the magnet. A change in the effective diameter of the coil of
only 5 mils could account for the total variation in the field.
The field homogeneity can also be affected by a misalignment of
the iron relative to the coil. The field was also measured at 2-
inch intervals and this measurement revealed a field structure with
a 6-inch period, corresponding to the length of a coil clamp
lamination packet.

End Field

The fringing field was measured on the axis of magnet E22-33.
The measurement was done with a Hall probe at 2005 A. From this
measurement the effective magnetic end was estimated at 2.96"
outside the edge of the lamination core.

Vertical Plane

The vertical magnetic plane was measured with a stretched wire.
A single-turn search coil was stretched through the warm bore using
a 4.0 mil tungsten wire. The width of the loop was maintained with
an accurately polished 1.0000-inch diameter quartz spacer at each
end. The plane of the search coil is rotated by synchronous step-
ping motors at each end, which have 20,000 steps per revolution,
and the angle is monitored by shaft encoders, which have a resolu-
tion of 32,768 counts per revolution.

A magnet under test is placed horizontally using precision
split levels, referencing from the outside surface of the iron
laminations. Then, also using split levels, the plane of the search

coil is placed vertically. The magnet is excited to a maximum
field and the output of the search coil is integrated. The non-
zero output of the search coil signifies rotation of the magnetic
vertical plane relative to the geometrical vertical plane. Then
the coil is rotated by predetermined values around the geometrical
vertical plane, and at each rotational position the magnet is ramp-
ed up and down. The output voltage of the coil is linear at these
small angles and is interpolated to give the zero-crossing angle,
which corresponds to the angle of the magnetic vertical plane.
The minimum resolution of the system is defined by that of the
stepping motor, which is about 0.3 milli-radian. The vertical
plane of E22-19 was measured to be off by about 0.1 degree from
its geometrical plane.

Integral Field

     To measure the integrated field value of the magnet the same
stretched wire device which was described earlier was used. After
that measurement the search coil plane is rotated by 90 degrees
from the magnetic vertical plane of the magnet under test.

     From that position the search coil is flipped by 180 degrees
to give the integrated remanent field value. The magnet is excited
and the output of the integrator gives the integrated field value
corresponding to that excitation. The output voltage of the inte-
grator and also that of the current shunt are measured with 5½-
digit DVM's (DANA 5900) for precision measurements.

     The integrated field value of magnet E22-33 was measured up
to 3000 A and its data is shown in Fig. 6. The ratio of the total
voltage, including remanent field effect, to the corresponding

current value is shown in that figure. The magnet was excited slowly from zero current to the maximum value and down to zero. The hysteresis effect, which is about 0.1% and is due to magnetization effect, is clearly shown. This value corresponds exactly to the hysteresis effect in the transfer function observed with NMR measurement[5].

The effective magnetic length, which was calculated from this measurement was 253.028 inches at 2000 A. It means the effective edge is 3.014 inches beyond the end of the iron yoke. This value matches reasonably well with the value measured with a Hall probe.

Hamonic Analysis of Magnetic Field

The 4-, 6-, 8-, and 10-pole coefficients of the magnetic field were measured directly using a harmonic coil and the 12- and 18-pole coefficients were extracted from the data for lower pole windings[3]. All coefficients were measured from 5 kG up to 40 kG. However, the magnetization of the superconductor produces a large hysteresis in the six-pole component at low field, and because of this, the 6-pole was measured down to 0.5 kG. The shape of each component shows only small changes from magnet to magnet, however, the absolute value does vary considerably. Both skew and normal coefficients were measured.

Due to symmetry, the 4-pole coefficients should not exist, but its presence can be explained by construction errors or off-centering of the coil. When off-centered, the 4-pole component has some error due to contributions from higher order harmonics, in particular the 6-pole which is the same order of magnetitude. The magnetic field can be reconstructed from the coefficients.

Figure 7 shows a plot of the percentage change in field ΔB/B in per cent as a function of the distance from the center of the mag- net along the horizontal axis. In this figure only 4-, 6-, 8-, and 10-poles were used.

Initially, only the 6-pole was measured in the end region, but on the most recent magnets other poles were measured. Only the normal 6- and 10-pole coefficients and skew 4- and 12-pole coefficients show any significant change at the ends.

PRODUCTION TEST FACILITY

The new test facility will consist of a cryogenic refrigera- tion system, a distribution system for the liquid Helium, and testing equipment. The layout of this facility is shown in Fig. 8. The refrigeration system is a CTI 1500, which has a compressor system, a cold box, and a control console. The compressor system consists of two oil-injected Sullair screw compressors, which are powered by a 200- and a 1000-horsepower motor, an oil separation system, and necessary instrumentation and controls. The refrigera- tor cold box contains four heat exchangers, two Sulzer gas-bearing turbo expanders, a small internal dewar, a JT valve, and control instrumentation. The control console with its flow diagram, indi- cators, alarms, and controllers allows one-man operation. Much of the operation of the refrigeration system will be monitored and controlled by a Texas Instrument 5TI Sequencer mounted on the con- trol console. The refrigeration system is designed to produce 330 liters of liquid Helium per hour at 4.4°K. Or it can provide 1250 watts of refrigeration at 21.5°K, 950 watts at 4.4°K, and 1.7 grams/ sec of liquid Helium for lead cooling.

The testing facility is designed so that liquid Helium from the CTI 1500 can be delivered directly to the distribution box or to a 10,000 ℓ storage dewar. It can collect here if a magnet is not being tested or it can be pumped to a magnet under test. There will be six testing stations, each with its own set of end boxes, transfer lines, and instrumentation. One will be dedicated to a standard magnet. Each can be operated totally independent of the others, but several can be receiving liquid at the same time. Others might have a magnet being installed, leak checked, or warming up. Eventually one or two of these testing stations will be devoted to quadrupole magnets.

The operation and monitoring of the distribution box, six magnet test stands and other components will be done by an independent LSI-11 microprocessor and CAMAC system and another 5TI system. These will be interfaced to the PDP-11 and CAMAC system now used for data taking of magnet tests.

The end box supplying helium is equipped with pressure indicators and temperature indicators in the nitrogen line and in the single phase and two-phase Helium lines. Also, helium level indicators are supplied for both single phase and two-phase helium lines. A heater is in the single phase line and VPT's are located in a steady state region on either end of the heater. This provides a method of calibration for measurements of heat leak into the single phase line. The return end box has a JT valve and is equipped with pressure indicators and VPT's in the liquid helium stream immediately before and after the JT valve. For heat loss measurement the warm bore cryostat, inserted into the magnet for field measurement, will

be filled up with liquid nitrogen to reduce heat loss through it.

The magnet is powered by a Transrex power supply built by Gulton Industries, Inc. The Transrex is an SCR controlled power supply capable of an output of 5000 A at 100 V. For a quench 70 to 90% of the magnet energy is dumped externally in a 0.2 ohm dump resistor. Data acquisition and manipulation is accomplished by an on-line computer (a PDP-11/10) and CAMAC system which has been developed specifically for this purpose.

It will take about eight hours to install and cool down a magnet, another eight hours to measure and test the magnet and another eight hours to warm it up. A magnet will be tested in one day, and the facility is designed to test three magnets a day.

ACKNOWLEDGEMENT

The authors would like to express their gratitude to all members of the Magnet Measurement Group who have contributed in different stages of this work. They also express their gratitude to C. Rode and his group for operation of the prototype satellite refrigerator.

REFERENCES

1.   The Fermilab Staff; The Energy Doubler: A Progress Report for the Energy Doubler/Saver Collider Project, June 1976.

2.   R. Yamada, H. Ishimoto, and M. E. Price; IEEE Trans. on Magnetics, MAG-13, No. 1, 86 (1976).

3.   R. Yamada, H. Ishimoto, and M. E. Price; IEEE Trans. on Nuclear Science, NS-24, No. 3, 1309 (1977).

4.   G. Kalbfleisch, P. J. Limon, and C. Rode; IEEE Trans. on Nuclear Science, NS-24, No. 3, 1239 (1977).

5.   R. Yamada, H. Ishimoto, M. F. Shea, and E. E. Schmidt; IEEE Trans. on Nuclear Science, NS-24, No. 3, 1312 (1977).

IRON YOKE
LAMINATION

LIQUID
NITROGEN

OUTER VACUUM TUBE

SINGLE PHASE
HELIUM

ROLLER SUSPENSION

CRYOSTAT VACUUM
SPACE FILLED WITH
MULTILAYER INSULATION

TWO PHASE
HELIUM

WIRE

COIL CLAMP
LAMINATION

BEAM VACUUM

INSULATION AND
VENTILATION
CHANNELS

CONTINUOUS SHIELD

STAND-OFF MOUNTING
RING

SCALE:

5"
4"
3"
2"
1"
0
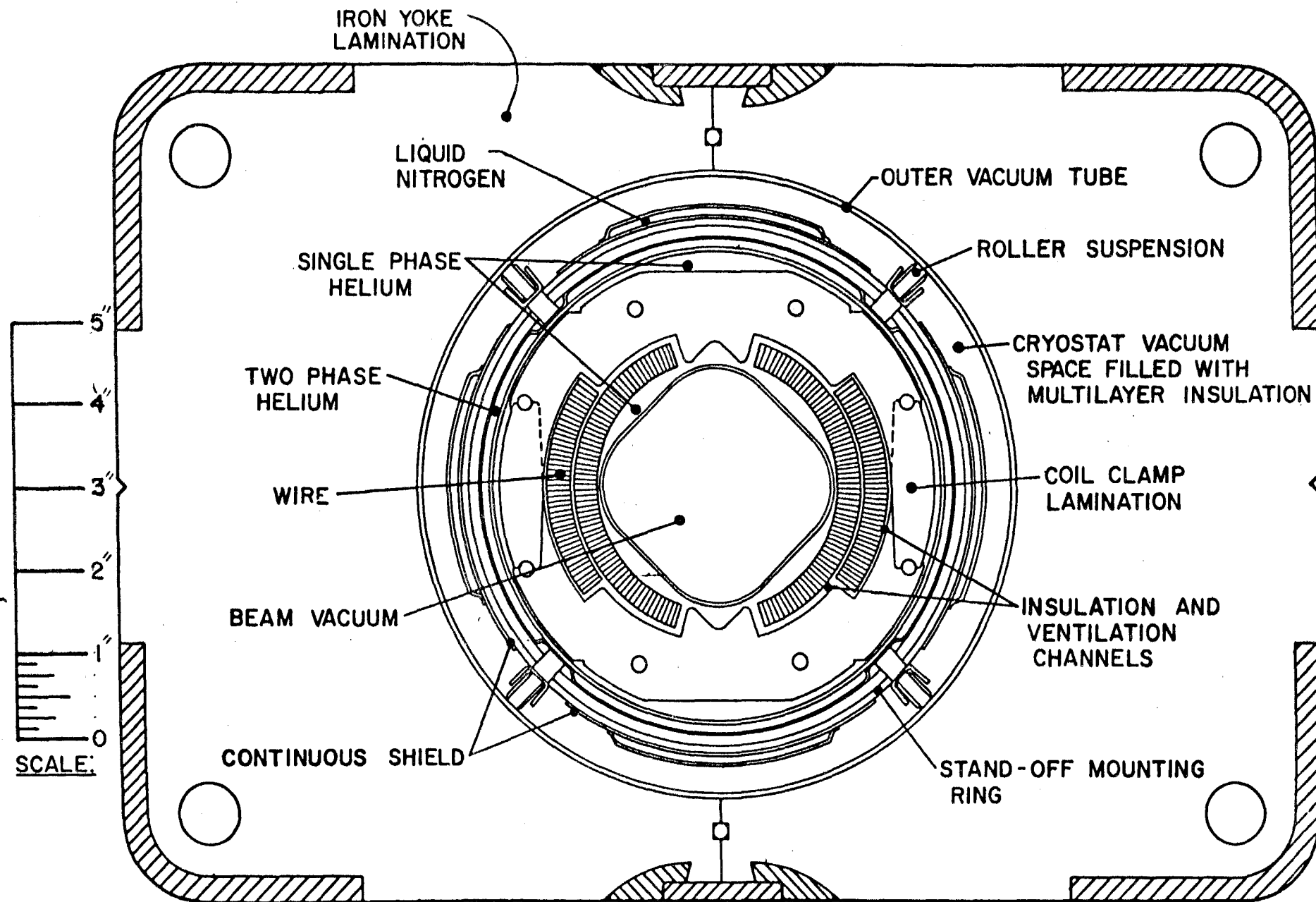
Fig. 1. Cross Sections of E22-14 Series Bending Magnets
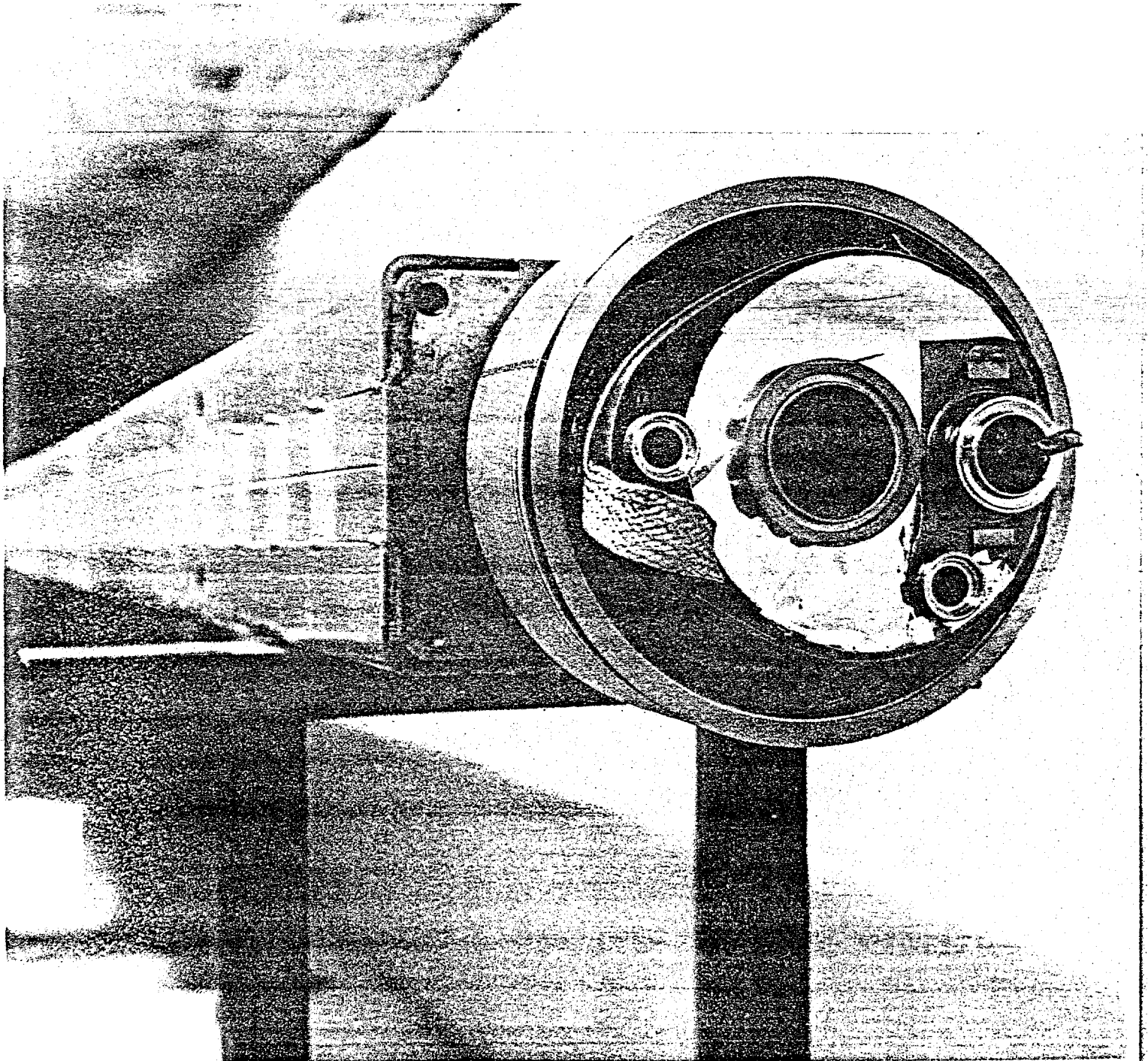
Fig. 2. End View of E22-14 Series Cryostat
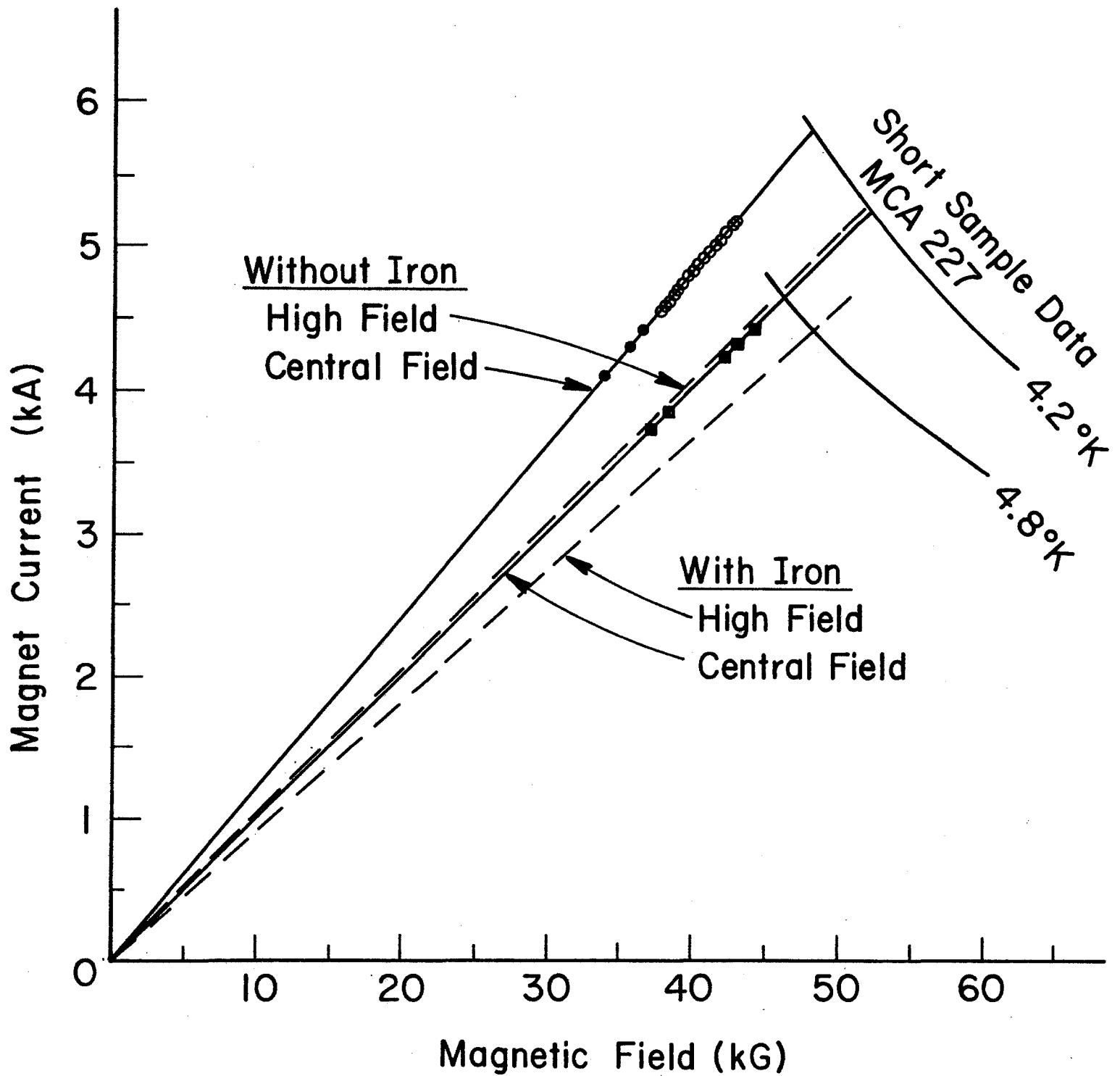
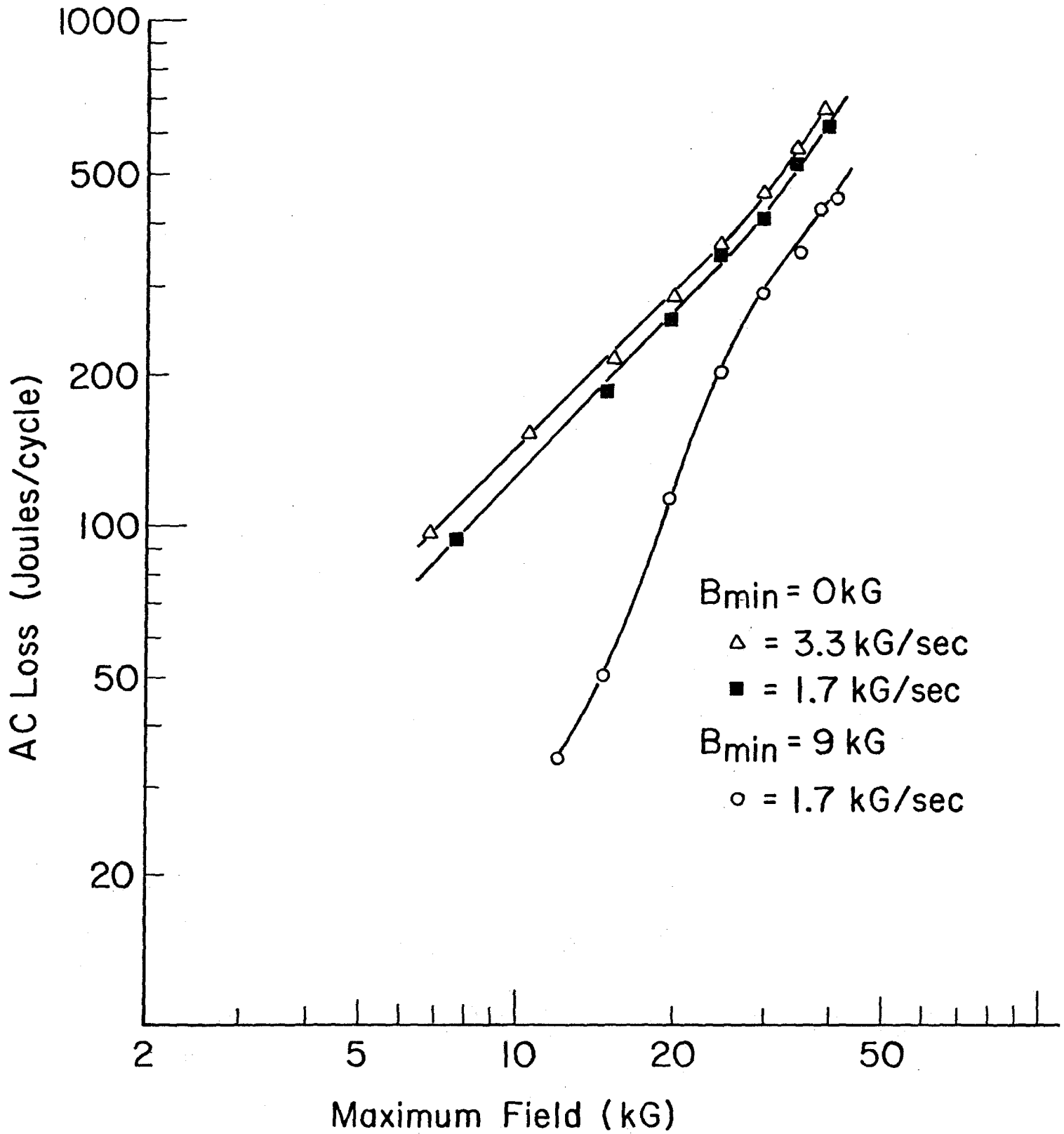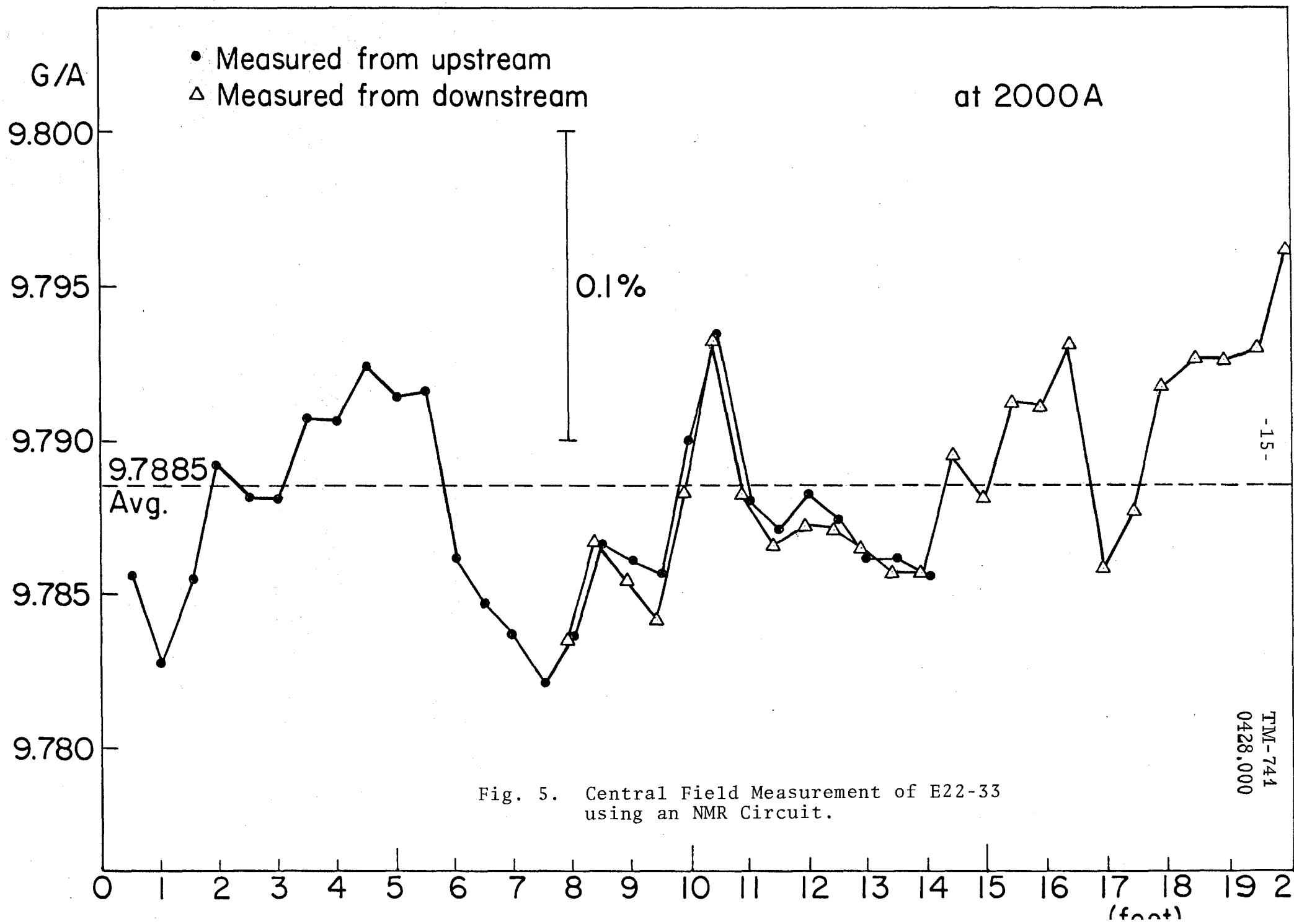Fig. 3.   Load Line and Quenches with and without Iron
for E22-19.

Fig. 4. AC Loss as a Function of Maximum
Field for E22-19.

Fig. 5. Central Field Measurement of E22-33
using an NMR Circuit.

-15-

TM-741
0428.000
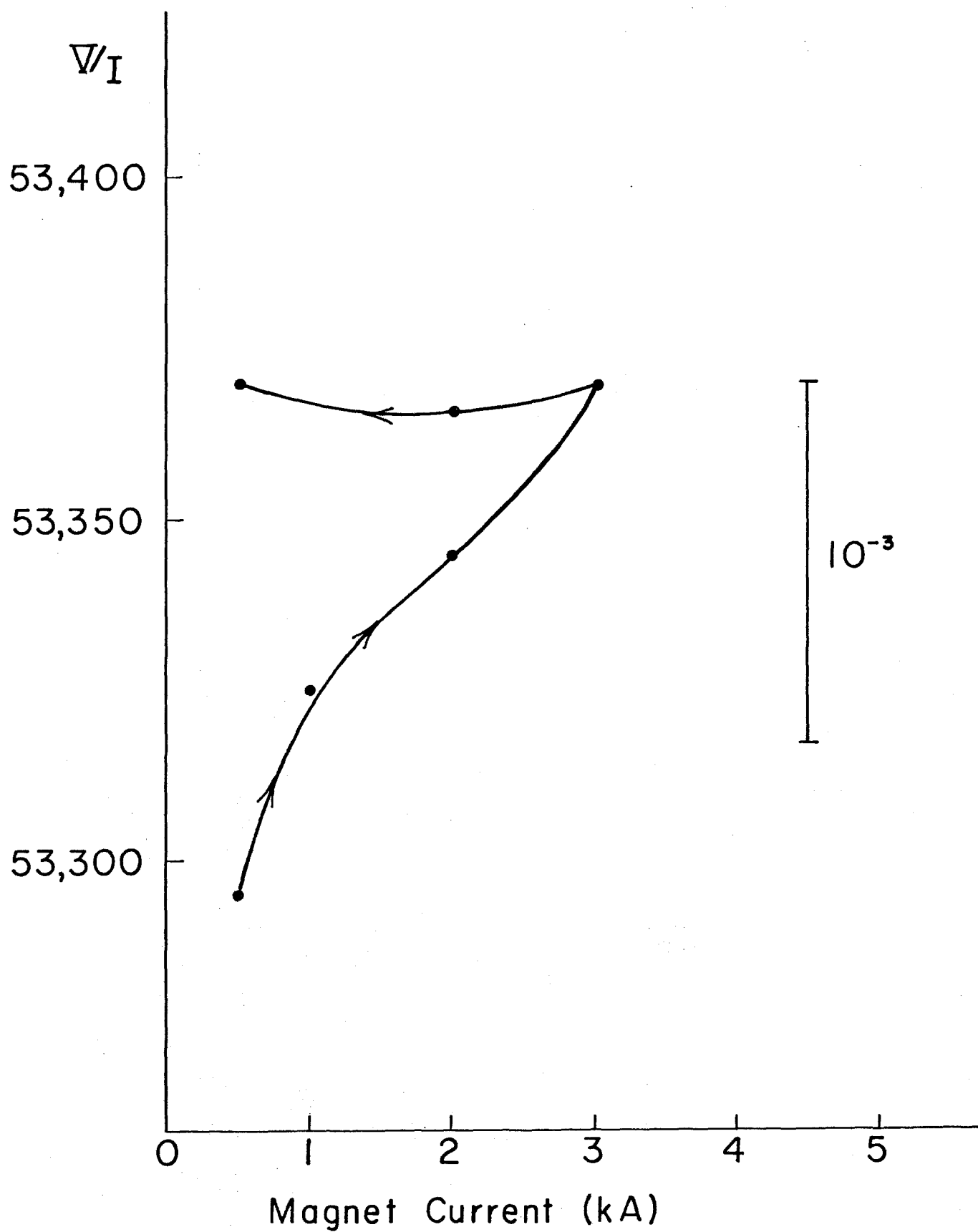
Fig. 6.   Integrated Field
Value of E22-33.
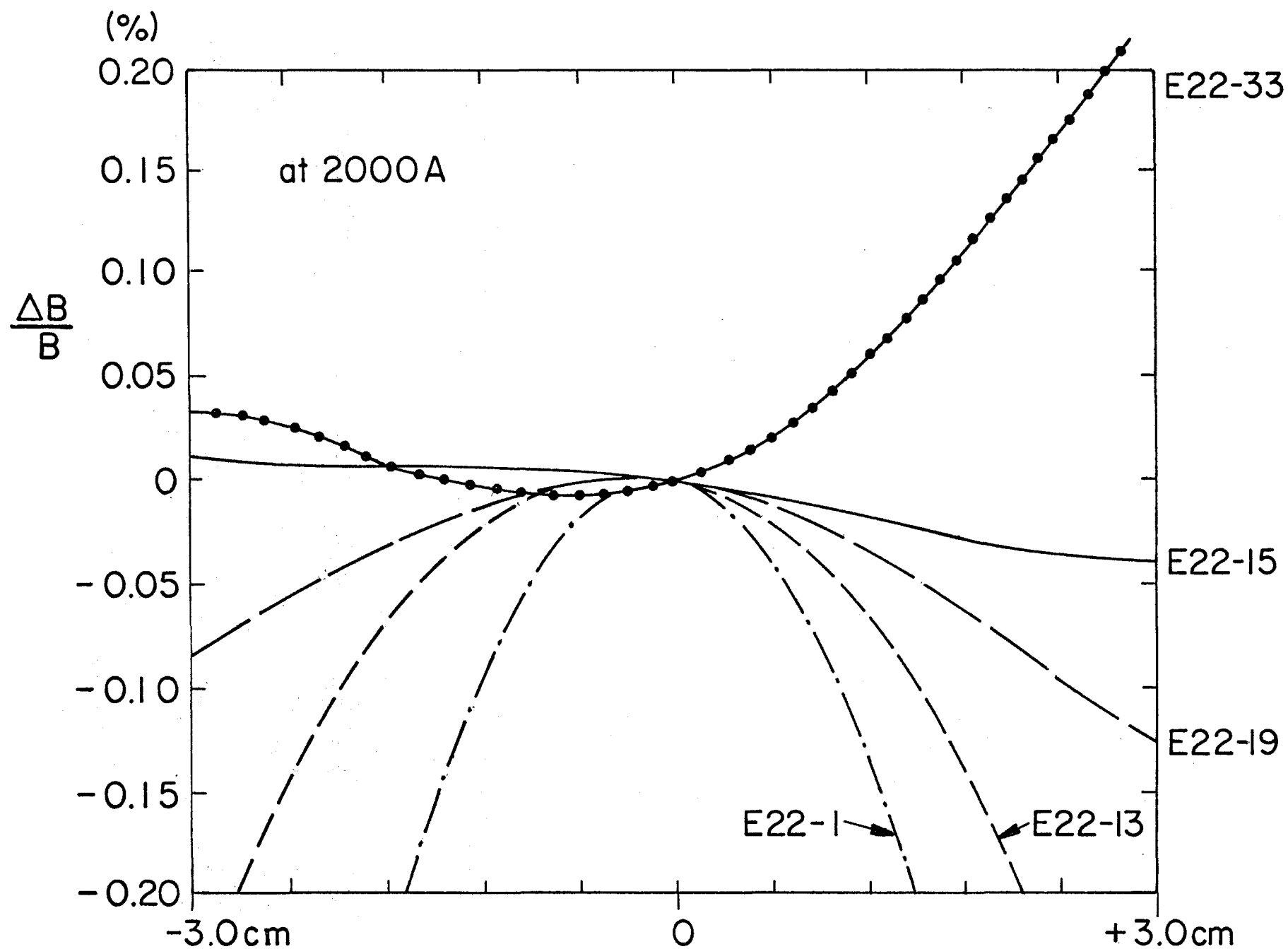
Fig. 7. Reconstruction of the Magnetic Field using 4-, 6-, 8-, and 10=pole Coefficients.
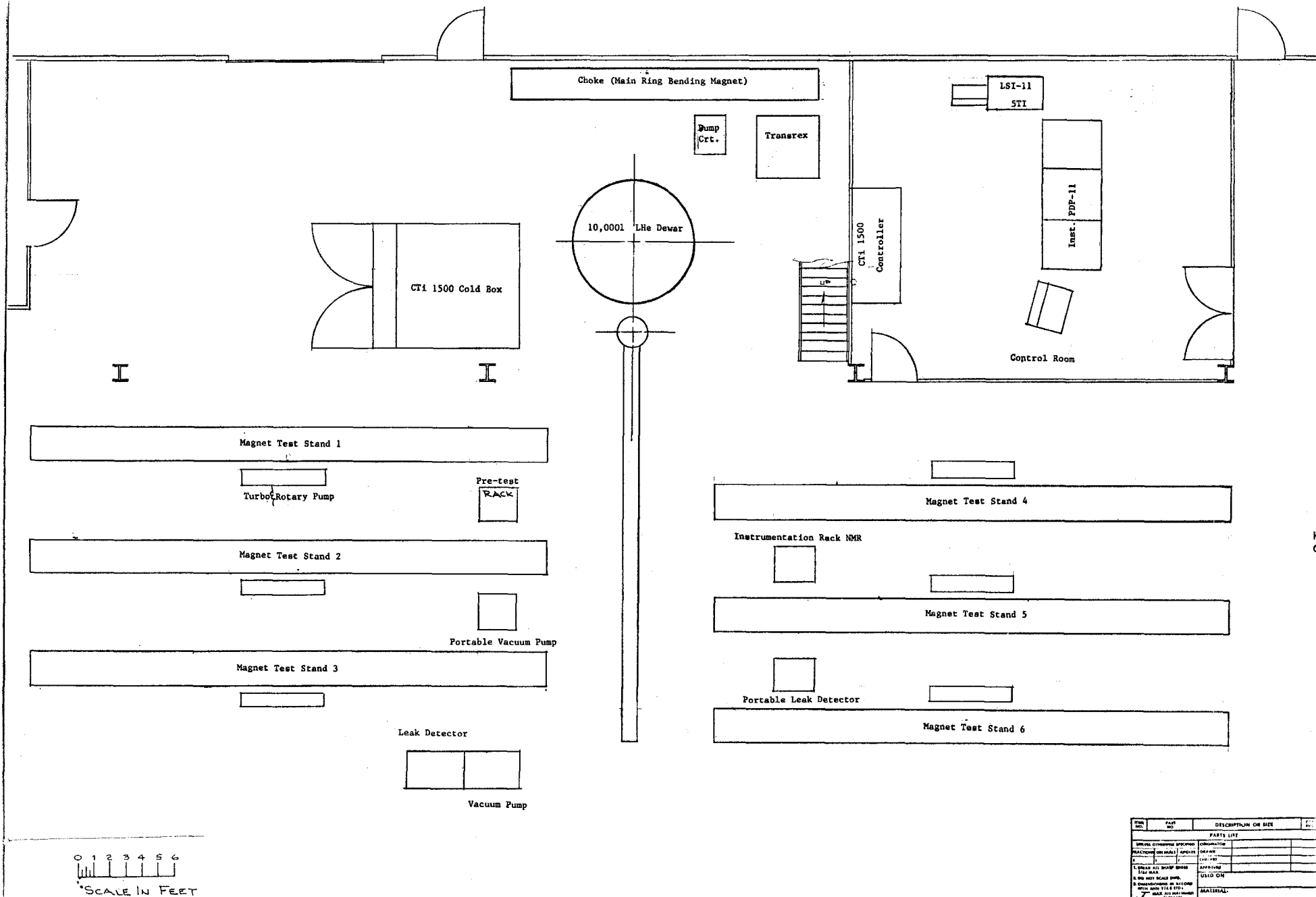
Fig. 8. Layout of Production Test Facility